Available online at www.sciencedirect.com
SCIENCE DIRECT
Neuropharmacology 49 (2005) 780–790
NEURO PHARMACOLOGY
www.elsevier.com/locate/neuropharm

A pincer-like configuration of TM2 in the human dopamine transporter is responsible for indirect effects on cocaine binding

Namita Sen [a,b], Lei Shi [c,d], Thijs Beuming [c], Harel Weinstein [c,d], Jonathan A. Javitch [a,b,*]

[a] *Center for Molecular Recognition and Departments of Psychiatry and Pharmacology, Columbia University College of Physicians and Surgeons, New York, NY 10032, USA*
[b] *New York State Psychiatric Institute, New York, NY 10032, USA*
[c] *Department of Physiology and Biophysics, Weill Medical College of Cornell University, 1300 York Avenue, New York, NY 10021, USA*
[d] *Institute for Computational Biomedicine, Weill Medical College of Cornell University, 1300 York Avenue, New York, NY 10021, USA*

Received 19 June 2005; received in revised form 18 August 2005; accepted 22 August 2005

Abstract

The second transmembrane segment (TM2) of DAT and other neurotransmitter transporters has been proposed to play a role in oligomerization as well as in cocaine binding. In an attempt to determine whether TM2 contributes to the binding site and/or transport pathway of DAT, we mutated to cysteine, one at a time, 25 residues in TM2 − from Phe98 to Gln122 − in an appropriate DAT background construct. Four of the mutants, F98C, G110C, P112C, and E117C, did not express at the cell surface, and G121C was inactive, despite its presence on the cell surface. Of the 21 mutants that expressed, none of the substituted cysteines reacted with MTSEA biotin-CAP, and none of the 20 functional mutants was sensitive to MTSEA or MTSET. Thus, TM2 does not appear to be water-accessible, based both on the lack of functional effects of charged MTS derivatives, and on the biochemical determination of lack of reaction with a biotinylated MTS derivative. This leads to the conclusion that TM2 does not contribute directly to the substrate-binding site or the transport pathway, and suggests that the observed effect of mutations in this region on cocaine binding is indirect. Three mutants, M106C, V107C and I108C, were crosslinked by treatment with $HgCl_2$. This crosslinking was inhibited by the presence of the cocaine analogue MFZ 2−12, likely due to a conformational rearrangement in TM2 upon inhibitor binding. However, the lack of crosslinking of cysteines substituted for Leu99, Leu113 and Leu120 − three of the residues that along with Met106 form a leucine heptad repeat in TM2 − makes it unlikely that this leucine repeat plays a role in symmetrical TM2 dimerization. Importantly, a high-resolution structure of LeuT, a sodium-dependent leucine transporter that is sufficiently homologous to DAT to suggest a high degree of structural similarity, became available while this manuscript was under review. We have taken advantage of this structure to explore further and interpret our experimental results in a rigorous structural context.

Keywords: Neurotransmitter transporter; Antidepressant; Cysteine substitution; Sulfhydryl reagents; Substituted cysteine accessibility method; Crosslinking

1. Introduction

The plasma membrane dopamine transporter (DAT) plays an essential role in terminating dopaminergic neurotransmission by reuptake of dopamine into presynaptic neurons (Giros and Caron, 1993). DAT is a member of the neurotransmitter: sodium symporter (NSS) family (2.A.22) (http://www.tcdb.org/tcdb/index.php?tc=2.A.22.1.3), which also includes transporters for serotonin, norepinephrine, GABA, glycine, several other amino acids, and osmolytes. DAT is a principal target for psychostimulant drugs such as cocaine and amphetamine (Kuhar et al., 1991; Ritz et al., 1987), and the serotonin and norepinephrine transporters are primary targets for antidepressant medications. The NSS are secondary active transporters that use electrochemical gradients to drive the translocation of organic substrates across membranes: sodium is co-transported with substrate and the sodium gradient is the major

* Corresponding author. Columbia University, P&S 11-401, Box 7, 630 West 168th Street, New York, NY 10032, USA. Tel.: +1 212 305 7308; fax: +1 212 305 5594.
E-mail address: jaj2@columbia.edu (J.A. Javitch).

0028-3908/$ - see front matter © 2005 Elsevier Ltd. All rights reserved.
doi:10.1016/j.neuropharm.2005.08.014

driving force for transport. These proteins are predicted to contain 12 TM domains and to have intracellular amino and carboxy termini (reviewed in Goldberg et al., 2003). Studies using specific antibodies and chemical modification have supported this topology for NSS members (Androutsellis-Theotokis and Rudnick, 2002; Chen et al., 1998; Ferrer and Javitch, 1998; Hersch et al., 1997).

Increasing evidence suggests that neurotransmitter transporters form dimers or oligomers in the plasma membrane (reviewed in Sitte et al., 2004). Mutations in a leucine heptad repeat in TM2 in both DAT and GAT1 disrupt oligomerization and interfere with cell surface expression (Scholze et al., 2002; Torres et al., 2003). A direct interaction of the leucine heptad repeat from TM2 of each protomer in a dimer has been inferred from these studies (Scholze et al., 2002; Torres et al., 2003), and a recent study has also implicated polar residues in TM2 in driving GAT1 oligomerization by intramembrane contacts of adjacent TM2 helices (Korkhov et al., 2004).

The present study investigates a potential role of TM2 in lining the transport pathway and/or binding site of DAT. Based on cysteine accessibility studies (Javitch, 1998; Karlin and Akabas, 1998; Stauffer and Karlin, 1994), we infer that TM2 is not water-accessible and does not contribute directly to the transport pathway or to the binding site for substrate or for cocaine. Although crosslinking of several residues in TM2 was observed in the presence of mercuric chloride, suggesting that TM2 may be located near a symmetric interface, the overall crosslinking pattern does not support a role of the leucine heptad repeat in TM2 in forming these contacts. Crosslinking of residues in TM2 was altered in the presence of a cocaine analog, consistent with state-dependent conformational changes in TM2 and with an indirect role of TM2 in cocaine binding. The high-resolution structure of LeuT, a sodium-dependent leucine transporter from *Aquifex aeolicus* (Yamashita et al., 2005) that is homologous to DAT, was released while this manuscript was under review. We have taken advantage of this structure to analyze our experimental results in a rigorous structural context.

2. Methods

2.1. Residue indexing

In addition to the residue positions in human DAT, we also use a common residue numbering scheme that facilitates comparison of the sequences of different NSS family members (Goldberg et al., 2003). Each generic residue number starts with the index of the transmembrane segment (TM), e.g. 2 for TM2, and is followed by a number indicating the position of the residue in the sequence, relative to a reference residue that is the most conserved position in that TM. The reference residue is arbitrarily assigned the number 50. For example, as our reference residue in TM2 we chose a conserved proline, the generic number of which would be 2.50, i.e. $Pro_{2.50}$. When referring to a particular transporter, the generic number can be preceded by the number of the residue in the particular sequence. In the human dopamine transporter, this proline in TM2 is at position 112, so this residue is referred to as $Pro112_{2.50}$. Accordingly, a glutamate residue located five amino acids C-terminal to $Pro112_{2.50}$ is designated $Glu117_{2.55}$. A similar numbering scheme had been developed for G-protein-coupled receptors (Ballesteros and Weinstein, 1995).

2.2. Mutagenesis, plasmid construction, transfection and cell culture

We used EM4 cells, human embryonic kidney 293 cells stably transfected with macrophage scavenger receptor to increase their adherence to tissue culture plastic (Robbins and Horlick, 1998). These were additionally stably transfected with a synthetic human DAT gene that was tagged at the amino terminus with a tandem epitope. The FLAG epitope was fused to the hemagglutinin epitope (FLAG–HA; 18 residues). The epitope tag replaced the first 22 amino acids of the protein and did not significantly affect expression or uptake (Khoshbouei et al., 2004; Saunders et al., 2000), or oligomerization (Hastrup et al., 2001, 2003). Mutations were made by polymerase chain reaction and confirmed by DNA sequencing. EM4 cells were grown in DMEM supplemented with 10% fetal bovine serum at 37 °C and 5% CO_2. Thirty-five-millimeter dishes of EM4 cells at 70–80% confluence were transfected with 2 μg of wild-type (WT) or mutant DAT cDNA in the bicistronic expression vector pCIHyg (Saunders et al., 2000) with 9 μl of Lipofectamine (Invitrogen) and 500 μl of Optimem (Invitrogen). Five hours after transfection, the solution was removed and fresh media added. Twenty-four hours after transfection the cells were split to a 100-mm dish and 250 μg/ml hygromycin (Invitrogen) was added to select for a stably transfected pool of cells.

2.3. Surface biotinylation and immunoblotting

EM4 cells stably expressing X2C (formerly referred to as "E2C"; Loland et al., 2004) or TM2 cysteine mutants in the X2C background were treated with cleavable Sulfo-NHS-SS-biotin (0.3 mg/ml in PBS, pH 9.0) (Pierce Chemical Co., Rockford, IL, USA) to label transporter on the cell surface. After biotinylation cells were incubated for 20 min at 4 °C in quenching buffer (20 mM Tris, 10 mM glycine, 140 mM NaCl, pH 7.4) followed by incubation with 10 mM *N*-ethylmaleimide (NEM) in PBS for 20 min at room temperature to alkylate free sulfhydryls. Cells were scraped into PBS–PI buffer (PBS supplemented with 1 μg/ml leupeptin, 1 μg/ml pepstatin, 2 μg/ml aprotinin, 2 μg/ml pefablock, and 10 mM *N*-ethylmaleimide). Cells were pelleted at 4 °C and incubated in PBS–PI supplemented with 0.2% digitonin at 4 °C for 20 min. Cells were pelleted and then incubated in lysis buffer (PBS–PI containing 1% Triton X-100) at 4 °C for 1 h with constant mixing. The extract was centrifuged at 4 °C (20,000 × *g*) for 30 min. An aliquot of the extract was removed for determination of total DAT. The remaining extract was incubated with 15 μl Neutravidin Plus beads (Pierce Chemical Co.) for 1 h at room temperature (for a 35-mm culture dish). The beads were washed twice with lysis buffer and then eluted with Laemmli sample buffer containing 50 mM dithiothreitol. The crude extracts and the eluted proteins were resolved by SDS-PAGE, transferred onto PVDF membranes (Millipore) and blocked for 1 h in 5% dry milk, 1% BSA, and 0.1% Tween-20 in TBS. FLAG-DAT was detected by anti-FLAG M2 primary antibody (Sigma) and antimouse-HRP secondary antibody (Santa Cruz Biotechnology, Inc.), with ECL-Plus (Amersham) and fluorescence detection and quantitation on a Fluoro-Chem imager using Alpha Ease™ FC software (Alpha Innotech Corporation, San Leandro, CA, USA).

2.4. Biotinylation of accessible cysteines

To label accessible cysteine residues, cells were washed twice with uptake buffer and incubated with 0.1 mM MTSEA biotin-CAP (2-((6-((biotinoyl)amino)hexanoyl)amino)ethyl-methanethiosulfonate) in uptake buffer, pH 7.4 for 10 min at room temperature. The reaction was stopped by aspiration and then by incubating with 10 mM NEM in PBS for 20 min at room temperature. Cells were harvested and lysed, the labeled proteins were isolated, and biotinylated DAT was detected as for Sulfo-NHS-SS-biotin labeling as described above.

2.5. Crosslinking

EM4 cells, stably transfected with the appropriate DAT construct, were seeded in a 60-mm plate and grown at 37 °C and 5% CO_2 for 48 h before an experiment. All cells were washed twice with uptake buffer (130 mM

NaCl, 1.3 mM KCl, 1.2 mM $MgSO_4$, 1.2 mM KH_2PO_4, 2.2 mM $CaCl_2$, 10 mM glucose, 10 mM Hepes, pH 7.4), and then reacted for 5 min at room temperature either with 1 mM Cu^{2+}(phenanthroline)$_4$ or with 20 μM $HgCl_2$ in uptake buffer. Pretreatment with 1 μM MFZ 2–12 was performed at RT for 20 min before crosslinking. The cells were washed twice with 2 ml of uptake buffer, and reacted for 20 min at RT with 10 mM NEM to block free sulfhydryl groups. The cells were scraped into uptake buffer–PI (uptake buffer supplemented with 2 μg/ml pefablock, 2 μg/ml aprotinin, 1 μg/ml leupeptin, 1 μg/ml pepstatin A and 10 mM NEM) and pelleted at 800 × *g* for 5 min at 4 °C. The pellet was suspended and incubated in 0.2% digitonin in uptake buffer–PI for 20 min at 4 °C. Cells were pelleted at 2000 × *g* for 10 min and stirred in 200 μl of 1% Triton X-100 in uptake buffer–PI (lysis buffer) per 60-mm plate at 4 °C for 1 h. The mixture was centrifuged at 14,000 × *g* for 30 min at 4 °C. Twenty micolitres of extract was mixed with an equal volume of 4× Laemmli sample buffer without reducing agent and held for 30 min at room temperature prior to SDS-PAGE and immunoblotting as above.

2.6. Uptake of [^{3}H]tyramine

The DAT substrate tyramine was used instead of dopamine for uptake assays since it is a substrate for DAT but not a substrate for endogenous catechol-*O*-methyl transferase, which has been shown to be present in human embryonic kidney 293 cells (Eshleman et al., 1997). EM4 cells, stably expressing the appropriate construct, were seeded in poly-D-lysine coated 96-well plates. After 48 h, the cells were washed three times with serum free DMEM, and incubated in serum free DMEM for 4 h at 37 °C and 5% CO_2. The cells were washed once with 200 μl uptake buffer and incubated in uptake buffer for 30 min at 37 °C. The uptake experiment was initiated by addition of 66 nM [^{3}H]tyramine (American Radiolabeled Chemicals, Inc.) in a final volume of 50 μl. Nonspecific uptake was determined in the presence of 2 mM tyramine. For determination of V_{max} and K_m values, increasing concentrations of tyramine (premixed with [^{3}H]tyramine) were added. After 5 min of incubation at room temperature, uptake was terminated by aspiration and washing twice with ice cold buffer. Cells were permeabilized with 50 μl of 1% Triton X-100 for 15 min. Two hundred microlitres of Optiphase Supermix scintillation fluid was added and radioactivity was determined in a Wallac 1450 microbeta counter. The IC_{50} for cocaine was determined similarly by incubating with increasing concentrations of cocaine (premixed with [^{3}H]tyramine).

2.7. Treatment with MTS reagents

For reaction with MTS reagents (Biotium or Toronto Research Chemicals) Cys-depleted DAT (CD-DAT) (Hastrup et al., 2001, 2003) and each of the TM2 cysteine mutants in the CD-DAT background were washed twice with uptake buffer and incubated with MTSEA ((2-aminoethyl)methanethiosulfonate) (0.25 mM) and MTSET ([2-(trimethylammonium)ethyl]methanethiosulfonate) (1 mM) at room temperature for 10 min. MTS reagents were freshly prepared in uptake buffer from a stock solution freshly prepared in water and maintained on ice. Cells were washed twice with PBS and transport activities were measured as described above.

3. Results

3.1. Transport activity of cysteine mutants

To generate a suitable human DAT background construct we replaced with Ala both Cys90 and Cys306, endogenous cysteines that we previously demonstrated to be accessible from the extracellular milieu (Chen et al., 2000b; Ferrer and Javitch, 1998). The resulting construct, X2C DAT (C90A/C306A), expressed well at the cell surface and had near-normal transport activity (Fig. 1A, Table 1; Loland et al., 2004). This X2C construct was used as the background for the creation of 25 cysteine substitution mutations in the predicted TM2. The transport

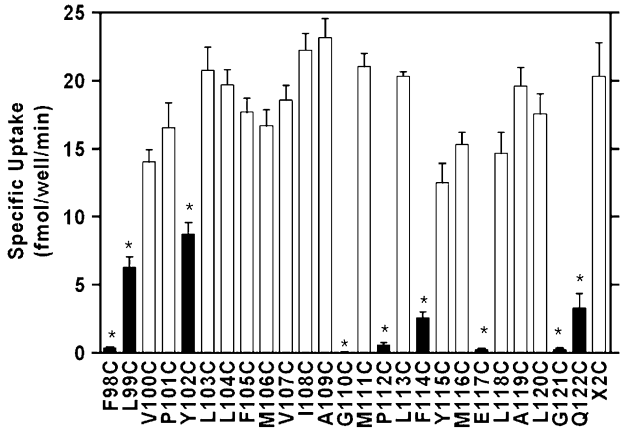

Fig. 1. Transport activity of EM4 cells transfected with X2C and TM2 cysteine mutants. [^{3}H]tyramine uptake by EM4 cells expressing X2C or the indicated mutants was measured as described in Section 2. Uptake was determined at 37 °C for 5 min. Nonspecific uptake was determined in the presence of 2 mM unlabeled tyramine. The data shown are the mean ± SEM of 3–4 experiments. Solid bars and * indicate mutants for which uptake was significantly different ($p < 0.05$) from that of X2C by one way ANOVA and Dunnett's test.

activity of the mutants varied substantially (Fig. 1A). Five mutants, including F98C, G110C, P112C, E117C, and G121C, were inactive. In L99C, Y102C, F114C, and Q122C, transport activity was substantially reduced, ranging from 13% to 43% of X2C. Transport activity in the remaining mutants ranged from 69% to 114% of X2C.

3.2. Surface expression

To measure cell surface expression we labeled cell surface DAT with Sulfo-NHS-SS-biotin, which reacts with surface lysines (Saunders et al., 2000). After separating the labeled proteins using Neutravidin beads, we quantified the maturely glycosylated surface DAT by immunoblot analysis. Whereas X2C and wild-type DAT are expressed at approximately similar levels on the surface (data not shown), the surface expression of the TM2 cysteine mutants varied widely compared to the background X2C construct (Fig. 2). No surface DAT was detected for four of the five inactive mutants, F98C, G110C, P112C, and E117C. In contrast, G121C expressed on the cell surface at 71% of the level of X2C despite the absence of transport activity in this mutant. Surface expression of L99C, Y102C, and M116C was 12%, 14%, and 34%, respectively, of that of X2C. Surface expression of the remaining mutants ranged from 60% to 149% of that of X2C.

An analysis of the ratio of transport activity to surface density showed that in many of the mutants transport activity tracked with changes in surface expression and, therefore, the ratio was similar to that of X2C. However, transport activity of L99C, Y102C, and M116C was substantially higher than expected given the low surface expression of these mutants in the face of relatively preserved transport. In contrast, transport activity per surface DAT was reduced more than 10-fold for F114C and Q122C, suggesting that these mutants were very inefficient at transport.

Table 1
Kinetic characteristics of TM2 cysteine mutants in the X2C background

Mutant	Tyramine K_m (μM)	Tyramine V_{max} (pmol/mg protein/min)	Cocaine IC_{50} (nM)
$F98_{2.36}C$	ND	ND	ND
$L99_{2.37}C$	8.3 ± 0.8	22.9 ± 1.7*	70 ± 20*
$V100_{2.38}C$	4.8 ± 0.4*	27.6 ± 3.5*	208 ± 33
$P101_{2.39}C$	5.0 ± 0.8*	40.8 ± 7.5	1575 ± 452
$Y102_{2.40}C$	9.6 ± 2.5	35.5 ± 12.6	109 ± 3*
$L103_{2.41}C$	9.7 ± 0.2	98.2 ± 9.9*	388 ± 21
$L104_{2.42}C$	4.0 ± 0.4*	35.2 ± 4.9	380 ± 60
$F105_{2.43}C$	3.2 ± 0.2*	28.3 ± 3.7*	1022 ± 192
$M106_{2.44}C$	0.7 ± 0.1*	7.2 ± 1.0*	219 ± 21
$V107_{2.45}C$	10.8 ± 1.0	86.3 ± 6.4	209 ± 29
$I108_{2.46}C$	2.2 ± 0.2*	20.1 ± 3.5*	711 ± 88
$A109_{2.47}C$	2.2 ± 0.4*	19.6 ± 4.4*	1420 ± 158
$G110_{2.48}C$	ND	ND	ND
$M111_{2.49}C$	4.3 ± 0.8*	48.8 ± 5.2	578 ± 16
$P112_{2.50}C$	ND	ND	ND
$L113_{2.51}C$	2.2 ± 0.2*	22.0 ± 2.7*	350 ± 42
$F114_{2.52}C$	1.4 ± 0.1*	1.3 ± 0.2*	1389 ± 296
$Y115_{2.53}C$	0.5 ± 0.1*	3.3 ± 1.3*	730 ± 9
$M116_{2.54}C$	3.8 ± 0.2*	29.2 ± 4.3*	304 ± 58
$E117_{2.55}C$	ND	ND	ND
$L118_{2.56}C$	2.9 ± 0.2*	20.6 ± 3.3*	909 ± 46
$A119_{2.57}C$	4.1 ± 0.6*	39.6 ± 6.0	619 ± 39
$L120_{2.58}C$	6.8 ± 0.9	62.2 ± 5.1	256 ± 27
$G121_{2.59}C$	ND	ND	ND
$Q122_{2.60}C$	0.1 ± 0.0	0.2 ± 0.0*	3680 ± 353*
X2C	9.3 ± 1.5	78.7 ± 7.7	645 ± 38

[^{3}H]tyramine uptake for EM4 cells expressing X2C or the indicated mutants was performed as described in Section 2. Uptake was performed using a range of concentration of unlabeled tyramine or cocaine (50 nM–100 μm) in competition with [^{3}H]tyramine. Nonspecific uptake was determined in the presence of 2 mM unlabeled tyramine. K_m, V_{max}, and cocaine IC_{50} were calculated using Prism 4 (GraphPad software). The data shown are the mean ± SEM of 3–4 experiments performed in duplicate. * indicates significantly different ($p < 0.05$) from X2C by one way ANOVA and Dunnett's test. ND indicates that the values could not be determined because of a lack of sufficient uptake for characterization.

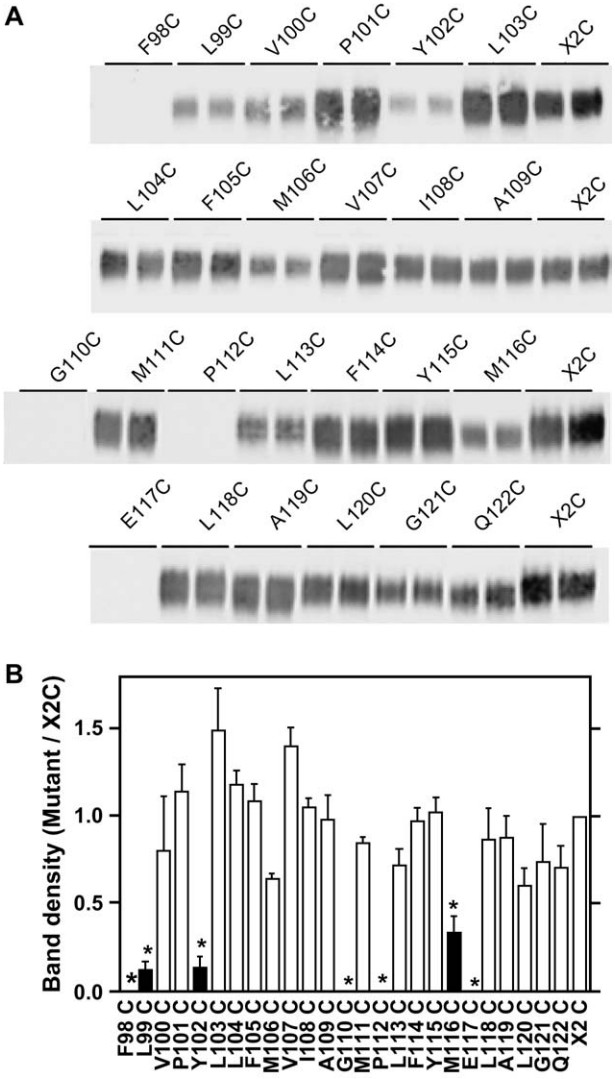

Fig. 2. Cell surface biotinylation of X2C and the TM2 cysteine mutants. EM4 cells expressing X2C and the indicated mutants were labeled with Sulfo-NHS-SS-biotin and processed as described in Section 2. Based on the relative integrated density of each ~90-kDa band, which represents the mature, fully glycosylated form of DAT, the expression levels of TM2 mutants are shown as a percentage of X2C expression. A. Duplicate bands from a representative experiment. B. The results shown are the mean ± SEM of 3–5 independent experiments. Solid bars and * indicate mutants for which surface expression was significantly different ($p < 0.05$) from that of X2C by one way ANOVA and Dunnett's test.

Since transport activity was determined from a single tracer concentration of [^{3}H]tyramine, we measured the tyramine concentration dependence for all 21 active mutants and compared them with X2C (Table 1). The K_m values for M106C, F114C, Y115C, and Q122C were reduced compared to that of X2C by 7-fold to over 100-fold. The V_{max} values for these four mutants were greatly decreased as well. The K_m and V_{max} values for the other mutants were generally similar to that of X2C.

The ratio of the V_{max} to the level of surface expression is proportional to the turnover number per surface DAT (Fig. 3). For M106C, F114C, Y115C, and Q122C, this analysis revealed a profound reduction in turnover number that cannot be accounted for by surface expression. Although we were unable to measure a V_{max} for G121C, its negligible transport activity despite near-normal surface expression (Fig. 2) suggests an even more extreme case of reduced turnover. In contrast, turnover was substantially increased for L99C and Y102C (Fig. 3).

3.3. Cocaine inhibition of transport

Cocaine inhibited tyramine uptake by each of the mutants (Table 1). The IC_{50} values of cocaine for F99C and Y102C were 9-fold and 6-fold lower, respectively, than that for X2C. The IC_{50} of cocaine was 6-fold higher for Q122C than that for X2C. The IC_{50} for cocaine inhibition was within 3-fold of that of X2C for all the other mutants.

3.4. Lack of water-accessibility of TM2 cysteines

It is possible that a cysteine could react with a sulfhydryl reagent without impairing uptake and thereby lead to a false negative determination of accessibility. Therefore, in order to perform a direct biochemical determination of the accessibility of the substituted cysteines in TM2, we reacted each

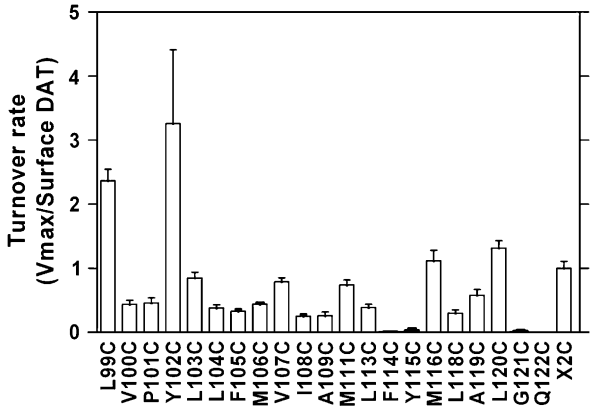

Fig. 3. Turnover rate of TM2 DAT mutants. Relative turnover rate was calculated as the V_{max}/relative surface DAT. V_{max} was measured as described in Table 1 and cell surface biotinylation was measured as described in Fig. 2. The data shown are the mean ± SEM of 3–4 experiments.

of the mutants with 100 μM MTSEA biotin-CAP. The X2C background did not react with MTSEA biotin-CAP under these conditions (Fig. 4). In contrast, a positive control, X2C in which the reactive 306C had been restored (X2C-306C), was highly labeled by this treatment (Fig. 4). Nonetheless, we detected no MTSEA biotin-CAP labeling for any of the TM2 mutants (data not shown).

Because it was conceivable that MTSEA biotin-CAP might be sterically excluded from a narrow crevice, we also performed functional analysis using the substituted cysteine accessibility method (SCAM) with smaller charged MTS derivatives (Stauffer and Karlin, 1994). These studies were performed in a Cys-depleted background (CD-DAT; Hastrup et al., 2001; see below) to decrease the possibility that residual endogenous cysteines might react and complicate the analysis. In the CD-DAT background, treatment with the

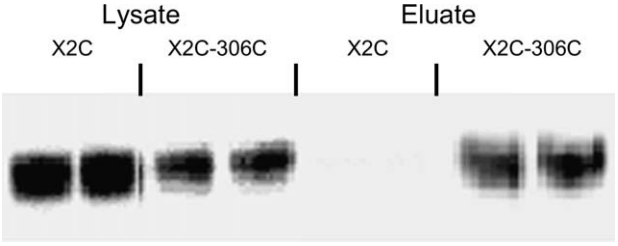

Fig. 4. Treatment with MTSEA biotin-CAP of X2C, X2C-306C and TM2 DAT mutants in the X2C background. Immunoblotting of lysate from cells treated with MTSEA biotin-CAP (100 μM, 10 min) after precipitation and elution from Neutravidin beads as described in Section 2. Lysates of X2C and X2C-306C protein showed bands at ~90 kDa. One hundred and thirty microlitres of each lysate X2C and X2C-306C was incubated with Neutravidin beads and eluted as described in Section 2. The eluate of X2C-306C revealed a single band at ~90 kDa indicating that 306C reacted with MTSEA biotin-CAP. In contrast, no biotinylation took place in X2C or in any of the TM2 cysteine mutants (blot not shown). The proteins were blotted with a M2 anti-FLAG antibody (Sigma) as described in Section 2.

positively charged MTS derivatives, MTSEA (0.25 mM) and MTSET (1 mM) failed to alter significantly tyramine uptake by any of the TM2 cysteine mutant (Fig. 5), consistent with the lack of accessibility of the substituted cysteines. Treatment with the negatively charged MTSES ((2-sulfonatoethyl)methanethiosulfonate)) (10 mM) also was without significant effect on tyramine uptake (data not shown).

3.5. Crosslinking of TM2 cysteine mutants

Because of previous results suggesting that TM2 of DAT and the homologous GABA transporter forms a symmetrical interface formed by a leucine zipper-like motif (Schmid et al., 2001; Scholze et al., 2002), we carried out crosslinking studies with the TM2 mutants to map a potential dimer interface. Previously we demonstrated two distinct symmetrical interfaces in DAT, one near the extracellular end of TM6 where Cys306 is crosslinked (Hastrup et al., 2001), and another in TM4 where Cys243 is crosslinked (Hastrup et al., 2003). Cys306 can be crosslinked oxidatively by Cu^{2+}(phenanthroline)$_4$ (CuP) and is crosslinked by mercuric ion as well. In contrast, Cys243 is crosslinked by mercuric ion but not by CuP. This is consistent with studies of the bacterial transporter

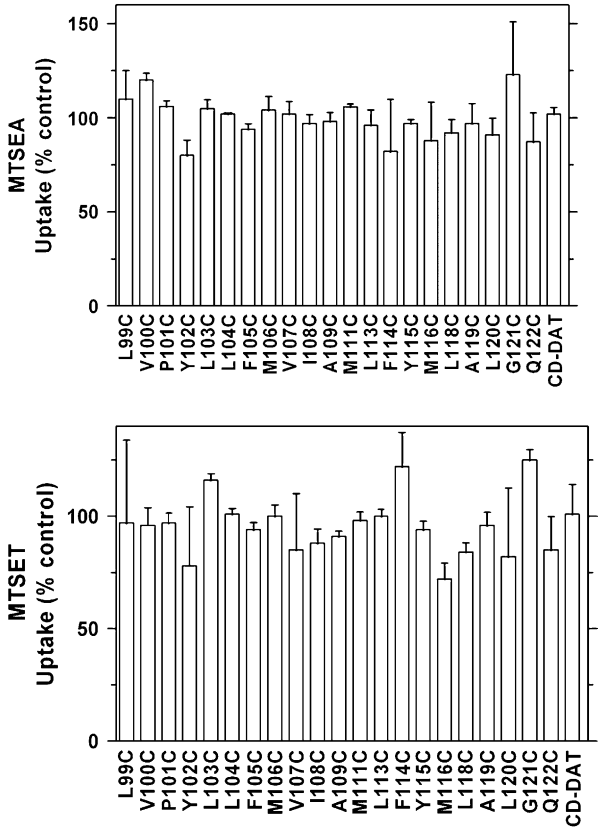

Fig. 5. Effects of MTSEA and MTSET on the transport activity of DAT TM2 cysteine mutants. EM4 cells expressing CD-DAT and the TM2 cysteine mutants in CD-DAT were treated with 0.25 mM MTSEA or 1 mM MTSET for 10 min, washed, and assayed for [^{3}H]tyramine transport as described in Fig. 1 and Section 2. The results are the mean ± SEM of 3–4 experiments.

EmrE in which a dimer interface in the transmembrane domain was crosslinked by mercuric ion (Soskine et al., 2002).

Preliminary experiments with the DAT TM2 cysteine mutants showed no crosslinking with CuP (data not shown). Because Cys243 is present in X2C, we would have been unable to interpret crosslinking experiments with mercuric ion in the X2C background. Therefore, we chose to pursue crosslinking experiments in the CD-DAT background that we have previously used for our crosslinking studies (Hastrup et al., 2001, 2003). This construct (FLAG–HA synDAT-C90A/C243A/C306A/C319M/C463S/C523A/C530A/C581L) contains no reduced cysteines in the extracellular or transmembrane regions. It does contain two extracellular cysteines that are thought to be disulfide bonded (Cys180 and Cys189) (Chen et al., 1997a; Wang et al., 1995) and two cysteines that we have shown to be intracellular (Cys135 and Cys342) (Ferrer and Javitch, 1998). Although surface expression and transport activity of CD-DAT are robust, the substitution of any of these four residual cysteines led to a profound loss of expression (data not shown). In contrast, Cys135 and Cys342 can be substituted individually or together in an X5C background (Ferrer and Javitch, 1998).

Each of the 25 TM2 cysteine substitution mutants was subcloned into the CD-DAT background and stably transfected pools of EM4 cells were created. For the five mutants that were inactive in the X2C background, no transport activity was observed in the CD-DAT background either. Transport activity was observed for all the other mutants. Curiously, however, several mutants showed substantially greater impairment of activity and expression in the CD-DAT background, consistent with our findings with mutating Cys135 and Cys342 in this background and with the difficulty of creating a cysteineless background construct.

As in the X2C background, no expression was detected in immunoblots for F98C, G110C, P112C, or E117C in the CD-DAT background. Immunoblotting of the other 21 mutants revealed maturely glycosylated monomer of ~90 kDa as well as varying amounts of immature transporter. Treatment with 1 mM CuP failed to crosslink any of these TM2 cysteine mutants in the CD-DAT background (data not shown). Twenty micromolar $HgCl_2$, however, crosslinked M106C, V107C, and I108C (Fig. 6). Crosslinking of these mutants was significantly reduced by treatment with the cocaine analog, MFZ 2–12 (Newman et al., 2001). Curiously, L103C did not crosslink in the absence of MFZ 2–12 but did crosslink to a small extent in the presence of the inhibitor (Fig. 6). No increases in crosslinking were seen in the presence of MFZ 2–12 in any of the other TM2 mutants (data not shown).

Met106 is part of the predicted leucine heptad repeat (Fig. 7A, B) inferred to form a symmetrical dimer interface (Scholze et al., 2002; Torres et al., 2003). However, cysteines substituted for Leu99, Leu113 and Leu120, which also contribute to this motif, were not crosslinked by CuP or by mercuric ion (data not shown), although we could detect maturely glycosylated transporter on immunoblots for each of these mutants and they expressed at the cell surface based on tyramine transport.

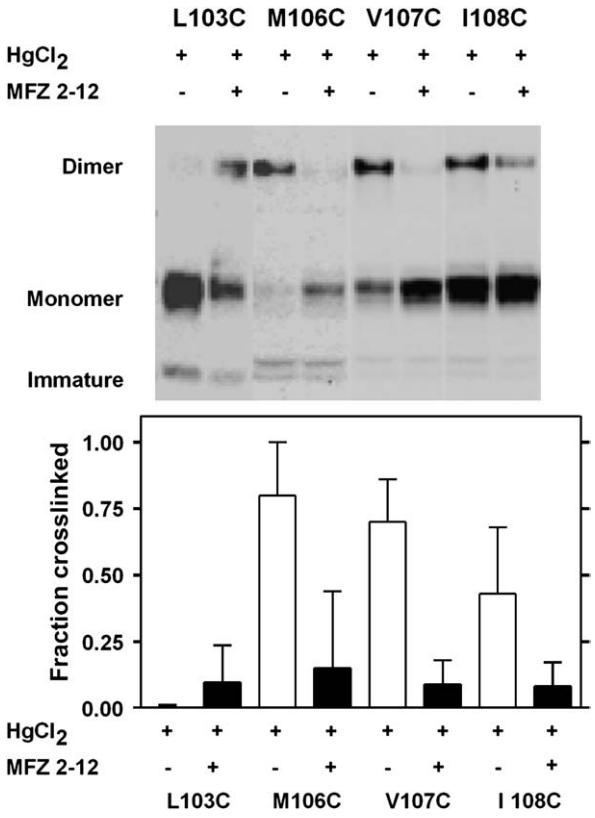

Fig. 6. Protection against and potentiation of DAT crosslinking by the cocaine analog MFZ 2–12. Crosslinking experiments were performed using EM4 cells expressing the indicated TM2 cysteine mutants in CD-DAT. Mutants were crosslinked with 20 μM $HgCl_2$ in the presence or in the absence of 1 μM MFZ 2–12. A. A representative blot is shown. B. The fraction crosslinked was calculated as the fraction of the total immunoreactivity in the monomer and dimer bands that was present in the dimer band. The results are the mean ± SEM of 3–5 independent experiments. Solid bars indicate mutants for which crosslinking was significantly different in the presence of MFZ 2-12 by paired t-test ($p < 0.05$).

4. Discussion

4.1. TM2 is not water-accessible

In the absence of a high-resolution structure of any NSS member, structural inferences about these transporters had been limited to those based on mutagenesis, affinity labeling and cysteine accessibility data (reviewed in Goldberg et al., 2003). Both TM1 and TM3 contain residues implicated in the binding of substrates and/or inhibitors, and a number of cysteine mutants in these TMs have been shown to be accessible in related NSS transporters as well as in DAT itself (Adkins et al., 2001; Barker et al., 1999, 1998; Chen and Rudnick, 2000a; Goldberg et al., 2003; Henry et al., 2003; Lee et al., 2000; Sato et al., 2004). TM2 has been inferred to play a role in cocaine binding based on mutagenesis studies (Chen et al., 2005; Wu and Gu, 2003). In addition, a number of DAT affinity labels have been shown to target a region containing TM1 and TM2 (Vaughan et al., 1999, 2001), leaving open a possible direct contribution of TM2 to the binding site in DAT.

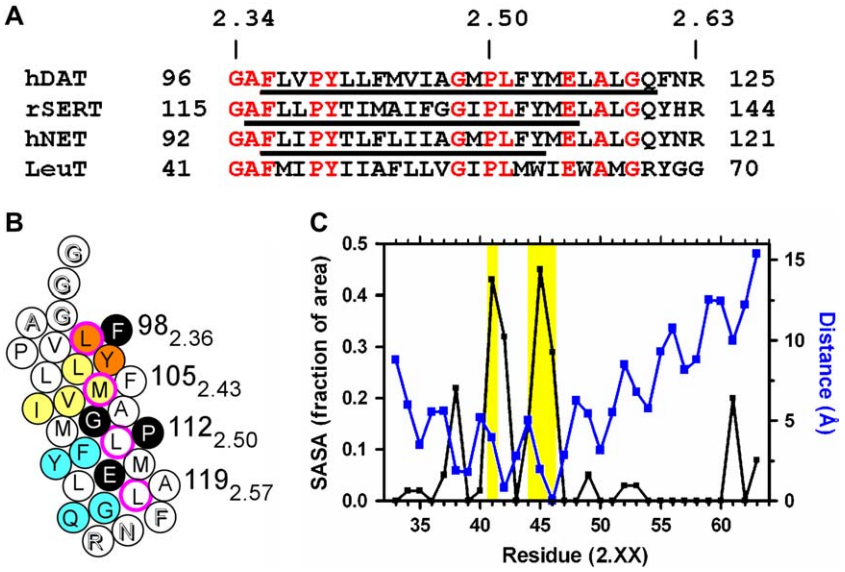

Fig. 7. Sequence alignment, helical net representation, and SASA analysis of TM2. A. The sequence corresponding to TM2 in the LeuT structure is aligned with the corresponding sequences of human DAT, rat SERT, and human NET. The residues that have been studied by the substituted cysteine accessibility method are underlined. Residues that are completely conserved in this alignment are shown in red font. B. Helical net representation. Cysteine substitution of residues shown as white on black prevented cell surface expression. Substitution of residues shown as black on orange or cyan led to decreased transport activity. After normalizing for surface DAT, for residues highlighted in orange, transport activity per surface DAT was increased, whereas for the residues in cyan, transport activity per surface DAT was decreased. The residues shown as black on yellow were crosslinked by mercuric chloride. The heavy purple circles show the residues in the leucine heptad repeat – note that the second position is substituted by a methionine in DAT. The extracellular end of TM2 is at the top of the figure. Residues at the extreme extracellular and intracellular ends shown in shadow font were not studied here but are predicted to be in the TM2 helix based on the LeuT structure (Yamashita et al., 2005). C. The fraction of solvent accessible surface area (SASA) for each residue in TM2 of LeuT was calculated using Insight II (Accelrys, San Diego) and is shown on the left axis in black. Using the LeuT coordinates, a distance calculation was made from the Cα of each residue to a plane perpendicular to the membrane, through the apex of the TM2 proline kink, and perpendicular to a plane defined by the two axes of the proline kink. This distance in angstroms is shown on the right axis in blue. The four positions for which the corresponding residues can be crosslinked in DAT are highlighted in yellow, showing that a combination of high SASA and low distance (proximity of two TM2 segments in the membrane) are necessary for crosslinking.

To explore such a possible role, we mapped systematically the contribution of TM2 to the water-accessible transport pathway and/or substrate-binding site of DAT using the substituted cysteine accessibility method (SCAM) (Javitch, 1998; Karlin and Akabas, 1998; Stauffer and Karlin, 1994). Treatment of the TM2 substituted cysteine mutants with MTSEA, MTSET or MTSES had no significant effect on tyramine transport (Fig. 5). However, it is possible for a cysteine to react with an MTS reagent but for this reaction to be without impact on transport, leading to a false negative conclusion of accessibility. Therefore, we also pursued a direct biochemical assessment of accessibility. For these studies we used MTSEA biotin-CAP (2-((6-((biotinoyl)amino)-hexanoyl)amino)ethyl-methanethiosulfonate), which has a long spacer arm, rather than the ''short-armed'' MTSEA biotin (2-((biotinoyl)amino)ethyl methanethiosulfonate), to increase the likelihood that the MTS moiety could gain access to a cysteine sulfhydryl in a water-accessible crevice within the transporter. In the dopamine D2 receptor we found previously that MTSEA biotin-CAP was able to react with Cys118 in the binding site crevice whereas MTS biotin could not (unpublished findings), presumably because the relatively bulky biotin moiety was sterically occluded from the crevice, whereas the long arm of the biotin-CAP reagent allowed the MTS moiety to reach and react with the accessible Cys118.

Although Cys306 near the extracellular end of TM6 was highly reactive with MTSEA biotin-CAP (Fig. 4), consistent with its accessibility to the extracellular milieu and its rapid reaction with MTSEA and MTSET (Ferrer and Javitch, 1998), no cysteines in TM2 were labeled by this reagent, consistent with the functional SCAM data and with the inference that TM2 does not line a water-accessible binding site or transport pathway. A similar lack of accessibility in TM2 also was observed in the homologous serotonin transporter (SERT) (Sato et al., 2004), and more recently in the norepinephrine transporter (NET) as well (Sucic and Bryan-Lluka, 2005) (see Fig. 7A).

4.2. An indirect role of TM2 in cocaine binding

A role for TM2 in cocaine binding has been suggested based on the ~70-fold loss of affinity of cocaine upon mutation of Leu104$_{2.42}$, Phe105$_{2.43}$, and Ala109$_{2.47}$ (Chen et al., 2005). In the X2C background, we found that mutation of these residues to Cys did not significantly affect the potency of cocaine, and these substituted cysteines did not react with MTS reagents, pointing to a buried location and to an indirect effect of mutations at these positions on cocaine binding. The structure of LeuT shows that the binding pocket for leucine and sodium involves residues from TM1, TM3, TM6 and TM8 (Yamashita et al., 2005) (Fig. 8A). TM2 is excluded from the substrate-binding site by TM1 and TM6 (Fig. 8A), helices that are broken in the middle by an unwound region

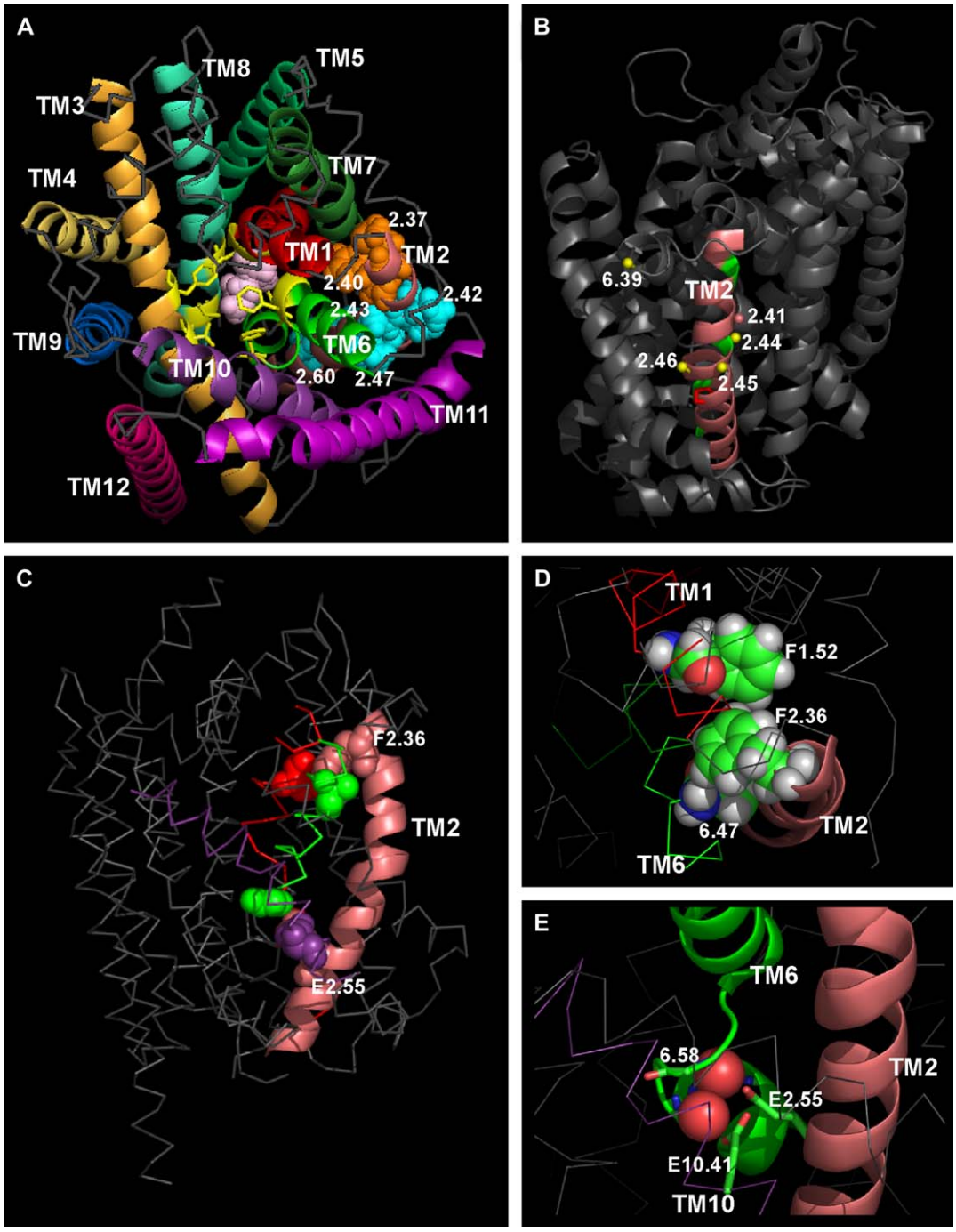

Fig. 8. Molecular representations of the structural context of TM2. A. LeuT structure (Yamashita et al., 2005) viewed from the extracellular side, showing the orientation of the 12 helices, each rendered in a different color. Leucine (in light pink) is shown in the binding pocket, comprising residues in TM1, TM3, TM6, and TM8. Residues in the leucine-binding pocket are indicated with yellow coloring of the ribbon, and contacting side chains are also shown, rendered as yellow sticks. TM2, shown in salmon color, is clearly screened from the binding pocket by TM1 and TM6 and makes extensive contacts with the backside of these helices. The residues for which mutation of the aligned residues in DAT *decreased* the affinity of cocaine are shown in cyan (Chen et al., 2005), and those for which mutation *increased* the affinity of cocaine are shown in orange (see text), both in space-filling rendering. B. A side view of LeuT with the aligned positions that crosslink in DAT indicated by yellow spheres at the Cβ position. These include three positions in TM2 as well as a residue at the C-terminal end of EL3 that is located on the same interface. (The one residue for which the aligned position in DAT crosslinks in the presence of a cocaine analog, but not in its absence, is shown as a salmon ball.) The positions of the leucines in the putative leucine zipper are indicated by green coloring of the ribbon. Note that they do not align on a face of TM2 and that the lower two residues face into the bundle as a result of the kink induced by the highly conserved $Pro_{2.50}$, which is shown in red. C. A side view of LeuT showing the pincer-like configuration of TM2 and the critical contacts it makes with TM1 and TM6 at the upper and lower pincer arms. D. A closer view of the upper pincer arm contacts shown in C. The $Phe43_{2.36}$ side chain is engaged in a stacking aromatic interaction with $Phe31_{1.52}$ and also interacts with the amide nitrogen of $Ala247_{6.47}$. These residues are shown in space-filling representation. E. A closer view of the lower pincer arm contacts shown in C. The highly conserved $Glu62_{2.55}$ contacts the amide nitrogen of $Gly258_{6.58}$ in the unwound region of TM6, as well as the carboxylate side chain of the highly conserved $Glu419_{10.41}$ in TM10 together with a water molecule, and the amide nitrogens of residues $Gly260_{6.60}$, $Ala261_{6.61}$, and $Ile262_{6.62}$ in TM6 through a second water molecule. The residues are shown in stick representation. These figures were prepared using Pymol (DeLano, W.L. http://www.pymol.org).

that has been implicated in the transport mechanism. This structure is consistent with our experimental evidence that TM2 of DAT does not contact the substrate-binding site directly, but instead makes extensive contacts with the ''backside'' of TM1 and TM6 that is opposite to the faces of these TMs that are directly involved in leucine and sodium binding.

It is very likely that the substrate-binding site in DAT and other NSS members is located in a similar position to that in LeuT. Although the location of the cocaine-binding site is not directly illuminated by the LeuT structure and will require further investigation, it seems most likely that cocaine binds in a position that overlaps the substrate-binding site (Chen et al., 1997b). However, 2.42, 2.43, and 2.47, the positions shown to decrease cocaine affinity (Chen et al., 2005) face the backside of TM6 (cyan in Fig. 8A) and their mutation likely perturbs the interaction of TM2 with TM6, and thereby is likely to affect ligand binding indirectly. In the current series of TM2 mutants, only $Q122_{2.60}C$, which lies at the cytoplasmic end of TM2, showed a substantially decreased potency of cocaine for inhibition of tyramine transport (Table 1). We hypothesize that the cocaine-binding site requires a configuration of DAT that is ''closed inward'', and that disruptions of the cytoplasmic side interactions required for this closure prevent the transporter from achieving the optimal cocaine-binding configuration. That this mechanism is likely to be similar to the indirect effects of mutation of $Tyr335_{6.68}$ on cocaine affinity (Loland et al., 2004) is also supported by the structure of LeuT. The aligned residue $Tyr268_{6.68}$ in LeuT has been suggested to participate in an internal gate (Yamashita et al., 2005). The likely mechanism for the substantially increased potency of cocaine in $L99_{2.37}C$ and $Y102_{2.40}C$ (Table 1) is also consistent with indirect effects of altering the interaction of TM2 with TM1 and TM6. From inspection of the LeuT structure we speculate that the mutation of these relatively bulky residues (orange in Fig. 8A) to cysteine might enable the transporter to reach more easily an ''open outward'' configuration, perhaps by allowing the upper parts of TM1 and TM6 to come closer to TM2, presumably at the same time maintaining the ''closed inward'' configuration. Interestingly, NET $Y98_{2.40}C$ also showed a substantially higher affinity for cocaine, suggesting that this structural mechanism may be shared among homologous transporters (Sucic and Bryan-Lluka, 2005).

4.3. Contacts with TM1 and TM6 enabled by the pincer-like configuration of TM2 are critical for function

Several highly conserved residues, including $Phe98_{2.36}$, $Gly110_{2.48}$, $Pro112_{2.50}$, and $Glu117_{2.55}$ did not tolerate mutation to cysteine. Similarly DAT $F98_{2.36}A$ (Lin et al., 1999), $P112_{2.50}A$ (Lin et al., 2000) and $E117_{2.55}Q$ (Chen et al., 2001) showed disrupted cell surface expression and no transport activity, as did $E113_{2.55}A$ and $E113_{2.55}D$ in NET (Sucic et al., 2002). An analysis of these loci in the LeuT structure reveals a number of highly conserved contacts. In LeuT, $Phe43_{2.36}$ contacts the highly conserved $Phe31_{1.52}$ (DAT $Phe86_{1.52}$) in TM1 and $Ala247_{6.47}$ (DAT $Ala314_{6.47}$) in TM6 (Fig. 8C, D). This contact is made possible by the kink in TM2, which is attributable to the highly conserved $Pro_{2.50}$, and creates the pincer-like configuration of TM2 in which the extracellular and intracellular ends of TM2 bend inwards toward the opposite ends of TM1 and TM6 (Fig. 8C). The conserved $Gly55_{2.48}$ (DAT $Gly110_{2.48}$) at i-2 from $Pro_{2.50}$ may enhance the local effect of the distortion due to the Pro-kink that exposes the i-4 and i-5 carbonyls which are not hydrogen bonded (Sansom and Weinstein, 2000) (rather than the more typical i-3 and i-4; Visiers et al., 2000), and this might explain the lack of expression of $G110_{2.48}C$ in DAT.

The lower arm of the TM2 pincer forms critical contacts at the cytoplasmic end, where the highly conserved $Glu62_{2.55}$ (DAT $Glu117_{2.55}$) contacts the amide nitrogen of $Gly258_{6.58}$ in the unwound region of TM6 (DAT $Gly325_{6.58}$), the carboxylate side chain of the highly conserved $Glu419_{10.41}$ (DAT $Glu491_{10.41}$) in TM10 together with a water molecule, and the amide nitrogens of residues $Gly260_{6.60}$, $Ala261_{6.61}$, and $Ile262_{6.62}$ in TM6 through a second water molecule (Fig. 8C, E). Although $G121_{2.59}C$ expressed at the surface, it did not transport. In LeuT the aligned $Gly66_{2.59}$ interacts with the backbone of the highly conserved $Ser267_{6.67}$ (DAT $Ser334_{6.67}$). Thus, the highly conserved TM2 residues that do not tolerate mutation in DAT appear critical to maintaining the kink in TM2 as well as the upper and lower interactions of the TM2 pincer arms.

4.4. The role of TM2 in oligomerization

Several NSS members have been shown to form constitutive oligomers in the plasma membrane (reviewed in Sitte et al., 2004). Together with the findings that mutations in a leucine heptad repeat in TM2 of DAT and of the GABA transporter interfered with cell surface expression and abolished the ability of these mutants to retain wild-type transporter intracellularly, these results suggested that residues in TM2 affect oligomerization, implicating the leucine repeat in the formation of a symmetrical interface (Scholze et al., 2002; Torres et al., 2003). In SERT, TM2 may also contribute to an oligomeric interface (Just et al., 2004).

Our findings were in contrast to previous results for DAT and GAT, as individual substitutions with cysteine of the residues in the leucine repeat, $Leu99_{2.37}$, $Met106_{2.44}$, $Leu113_{2.51}$, and $Leu120_{2.58}$, were well tolerated and the mutant transporters reached the cell surface and transported tyramine. Although $M106_{2.44}C$ was crosslinked by $HgCl_2$, none of the other positions in the leucine repeat was crosslinked, either in the presence or in the absence of the cocaine analog, MFZ 2–12. Thus, although our findings are consistent with the location of TM2 near a symmetrical interface, the lack of crosslinking at three of the four positions is difficult to reconcile with a classical role for the leucine heptad repeat. While the leucines in the ''zipper'' might appear on a helical net to be positioned on the same face of the helix (Fig. 7B), the face shift associated with a Pro-kink (Sansom and Weinstein, 2000; Visiers et al., 2000) was shown to produce significant

reorientations that interfere with helix–helix interactions (Carter et al., 1998). This likely results from the highly conserved $Pro_{2.50}$-induced kink in TM2, which orients $Leu_{2.51}$ and $Leu_{2.58}$ inwards (green in Fig. 8B).

Analysis of the solvent accessible surface area of residues in TM2 of LeuT reveals that approximately its entire lower half is not solvent accessible, because it is buried by intracellular loops and neighboring helices (Fig. 7C). Of the residues in TM2 that remains solvent accessible, those located near the Pro-kink are positioned so that they could crosslink with the corresponding residues in a second protomer. It is important to note that these contacts are made possible by the pincer-like configuration of TM2 (Fig. 8B). It seems likely that the changes in crosslinking upon binding of cocaine analogs result from a conformational rearrangement of TM2, possibly around the flexible hinge of the Pro-kink (Sansom and Weinstein, 2000).

We have previously shown that DAT can be crosslinked at two distinct symmetrical interfaces, Cys306 near the extracellular end of TM6 and Cys243 in TM4 (Hastrup et al., 2001, 2003). We therefore inferred that DAT exists in the plasma membrane as a dimer of dimers. This proposal is consistent with radiation inactivation data suggesting a tetrameric structure for DAT (Milner et al., 1994), although other findings using this approach were consistent with dimer (Berger et al., 1994). That $L103_{2.41}C$ crosslinks more in the presence of MFZ 2–12 argues against a change of the oligomerization state of DAT upon binding of the cocaine analog and instead for a conformational change in TM2. Notably, in the LeuT structure, $Lys239_{6.39}$, which aligns with DAT $Cys306_{6.39}$, is located near the C-terminal end of the third extracellular loop (EL3) in a distorted turn of helix that lies on the same face as the patch of residues in TM2 that are crosslinked (Fig. 8B). Thus, it appears likely that these residues form a common interface that is distinct from the TM4 interface.

Although the location of these crosslinked residues is consistent with their accessibility in the LeuT structure, it remains unclear whether the crosslinking occurs at a fixed oligomerization interface, or from trapping of mobile DAT protomers in the membrane. The additional investigation required to clarify the dynamics of the crosslinking will be aided by the availability of the LeuT structure and the possibility of addressing specific structural hypotheses. The crystal structure of LeuT revealed a dimer interface involving TM9 and TM12 (Yamashita et al., 2005), but the relevance of this interface to the organization of LeuT in the native membrane, as well as the relevance of this potential configuration to other NSS family members will require additional investigation as well.

Acknowledgements

This work was supported by National Institutes of Health grants R01 DA11495, P01 DA12408, K02 MH57324 and K05 DA00060.

References

Adkins, E.M., Barker, E.L., Blakely, R.D., 2001. Interactions of tryptamine derivatives with serotonin transporter species variants implicate transmembrane domain I in substrate recognition. Mol. Pharmacol. 59, 514–523.

Androutsellis-Theotokis, A., Rudnick, G., 2002. Accessibility and conformational coupling in serotonin transporter predicted internal domains. J. Neurosci. 22, 8370–8378.

Ballesteros, J., Weinstein, H., 1995. Integrated methods for the construction of three-dimensional models of structure–function relations in G protein-coupled receptors. Methods Neurosci. 25, 366–428.

Barker, E.L., Moore, K.R., Rakhshan, F., Blakely, R.D., 1999. Transmembrane domain I contributes to the permeation pathway for serotonin and ions in the serotonin transporter. J. Neurosci. 19, 4705–4717.

Barker, E.L., Perlman, M.A., Adkins, E.M., Houlihan, W.J., Pristupa, Z.B., Niznik, H.B., Blakely, R.D., 1998. High affinity recognition of serotonin transporter antagonists defined by species-scanning mutagenesis. An aromatic residue in transmembrane domain I dictates species-selective recognition of citalopram and mazindol. J. Biol. Chem. 273, 19459–19468.

Berger, S.P., Farrell, K., Conant, D., Kempner, E.S., Paul, S.M., 1994. Radiation inactivation studies of the dopamine reuptake transporter protein. Mol. Pharmacol. 46, 726–731.

Carter, J., Gragerov, A., Konvicka, K., Elder, G., Weinstein, H., Lazzarini, R.A., 1998. Neurofilament (NF) assembly; divergent characteristics of human and rodent NF-L subunits. J. Biol. Chem. 273, 5101–5108.

Chen, J.G., Liu-Chen, S., Rudnick, G., 1997a. External cysteine residues in the serotonin transporter. Biochemistry 36, 1479–1486.

Chen, J.G., Sachpatzidis, A., Rudnick, G., 1997b. The third transmembrane domain of the serotonin transporter contains residues associated with substrate and cocaine binding. J. Biol. Chem. 272, 28321–28327.

Chen, J.G., Liu-Chen, S., Rudnick, G., 1998. Determination of external loop topology in the serotonin transporter by site-directed chemical labeling. J. Biol. Chem. 273, 12675–12681.

Chen, J.G., Rudnick, G., 2000a. Permeation and gating residues in serotonin transporter. Proc. Natl. Acad. Sci. U.S.A. 97, 1044–1049.

Chen, N., Ferrer, J.V., Javitch, J.A., Justice Jr., J.B., 2000b. Transport-dependent accessibility of a cytoplasmic loop cysteine in the human dopamine transporter. J. Biol. Chem. 275, 1608–1614.

Chen, N., Vaughan, R.A., Reith, M.E., 2001. The role of conserved tryptophan and acidic residues in the human dopamine transporter as characterized by site-directed mutagenesis. J. Neurochem. 77, 1116–1127.

Chen, R., Han, D.D., Gu, H.H., 2005. A triple mutation in the second transmembrane domain of mouse dopamine transporter markedly decreases sensitivity to cocaine and methylphenidate. J. Neurochem. 94, 352–359.

Eshleman, A.J., Stewart, E., Evenson, A.K., Mason, J.N., Blakely, R.D., Janowsky, A., Neve, K.A., 1997. Metabolism of catecholamines by catechol-*O*-methyltransferase in cells expressing recombinant catecholamine transporters. J. Neurochem. 69, 1459–1466.

Ferrer, J.V., Javitch, J.A., 1998. Cocaine alters the accessibility of endogenous cysteines in putative extracellular and intracellular loops of the human dopamine transporter. Proc. Natl. Acad. Sci. U.S.A. 95, 9238–9243.

Giros, B., Caron, M.G., 1993. Molecular characterization of the dopamine transporter. Trends Pharmacol. Sci. 14, 43–49.

Goldberg, N.R., Beuming, T., Soyer, O.S., Goldstein, R.A., Weinstein, H., Javitch, J.A., 2003. Probing conformational changes in neurotransmitter transporters: a structural context. Eur. J. Pharmacol. 479, 3–12.

Hastrup, H., Karlin, A., Javitch, J.A., 2001. Symmetrical dimer of the human dopamine transporter revealed by cross-linking Cys-306 at the extracellular end of the sixth transmembrane segment. Proc. Natl. Acad. Sci. U.S.A. 98, 10055–10060.

Hastrup, H., Sen, N., Javitch, J.A., 2003. The human dopamine transporter forms a tetramer in the plasma membrane: cross-linking of a cysteine in the fourth transmembrane segment is sensitive to cocaine analogs. J. Biol. Chem. 278, 45045–45048.

Henry, L.K., Adkins, E.M., Han, Q., Blakely, R.D., 2003. Serotonin and cocaine-sensitive inactivation of human serotonin transporters by

methanethiosulfonates targeted to transmembrane domain I. J. Biol. Chem. 278, 37052–37063.

Hersch, S.M., Yi, H., Heilman, C.J., Edwards, R.H., Levey, A.I., 1997. Subcellular localization and molecular topology of the dopamine transporter in the striatum and substantia nigra. J. Comp. Neurol. 388, 211–227.

Javitch, J.A., 1998. Probing structure of neurotransmitter transporters by substituted-cysteine accessibility method. Methods Enzymol. 296, 331–346.

Just, H., Sitte, H.H., Schmid, J.A., Freissmuth, M., Kudlacek, O., 2004. Identification of an additional interaction domain in transmembrane domains 11 and 12 that supports oligomer formation in the human serotonin transporter. J. Biol. Chem. 279, 6650–6657.

Karlin, A., Akabas, M.H., 1998. Substituted-cysteine accessibility method. Methods Enzymol. 293, 123–145.

Khoshbouei, H., Sen, N., Guptaroy, B., Johnson, L., Lund, D., Gnegy, M.E., Galli, A., Javitch, J.A., 2004. N-terminal phosphorylation of the dopamine transporter is required for amphetamine-induced efflux. PLoS Biol. 2, 0387–0393.

Korkhov, V.M., Farhan, H., Freissmuth, M., Sitte, H.H., 2004. Oligomerization of the {gamma}-aminobutyric acid transporter-1 is driven by an interplay of polar and hydrophobic interactions in transmembrane helix II. J. Biol. Chem. 279, 55728–55736.

Kuhar, M.J., Ritz, M.C., Boja, J.W., 1991. The dopamine hypothesis of the reinforcing properties of cocaine. Trends Neurosci. 14, 299–302 (Review).

Lee, S.H., Chang, M.Y., Lee, K.H., Park, B.S., Lee, Y.S., Chin, H.R., 2000. Importance of valine at position 152 for the substrate transport and 2beta-carbomethoxy-3beta-(4-fluorophenyl)tropane binding of dopamine transporter. Mol. Pharmacol. 57, 883–889.

Lin, Z., Itokawa, M., Uhl, G.R., 2000. Dopamine transporter proline mutations influence dopamine uptake, cocaine analog recognition, and expression. FASEB J. 14, 715–728.

Lin, Z., Wang, W., Kopajtic, T., Revay, R.S., Uhl, G.R., 1999. Dopamine transporter: transmembrane phenylalanine mutations can selectively influence dopamine uptake and cocaine analog recognition. Mol. Pharmacol. 56, 434–447.

Loland, C.J., Granas, C., Javitch, J.A., Gether, U., 2004. Identification of intracellular residues in the dopamine transporter critical for regulation of transporter conformation and cocaine binding. J. Biol. Chem. 279, 3228–3238.

Milner, H.E., Beliveau, R., Jarvis, S.M., 1994. The in situ size of the dopamine transporter is a tetramer as estimated by radiation inactivation. Biochim. Biophys. Acta 1190, 185–187.

Newman, A.H., Zou, M.F., Ferrer, J.V., Javitch, J.A., 2001. [3H]MFZ 2–12: a novel radioligand for the dopamine transporter. Bioorg. Med. Chem. Lett. 11, 1659–1661.

Ritz, M.C., Lamb, R.J., Goldberg, S.R., Kuhar, M.J., 1987. Cocaine receptors on dopamine transporters are related to self-administration of cocaine. Science 237, 1219–1223.

Robbins, A.K., Horlick, R.A., 1998. Macrophage scavenger receptor confers an adherent phenotype to cells in culture. Biotechniques 25, 240–244.

Sansom, M.S., Weinstein, H., 2000. Hinges, swivels and switches: the role of prolines in signalling via transmembrane alpha-helices. Trends Pharmacol. Sci. 21, 445–451.

Sato, Y., Zhang, Y.W., Androutsellis-Theotokis, A., Rudnick, G., 2004. Analysis of transmembrane domain 2 of rat serotonin transporter by cysteine scanning mutagenesis. J. Biol. Chem. 279, 22926–22933.

Saunders, C., Ferrer, J.V., Shi, L., Chen, J., Merrill, G., Lamb, M.E., Leeb-Lundberg, L.M., Carvelli, L., Javitch, J.A., Galli, A., 2000. Amphetamine-induced loss of human dopamine transporter activity: an internalization-dependent and cocaine-sensitive mechanism. Proc. Natl. Acad. Sci. U.S.A. 97, 6850–6855.

Schmid, J.A., Scholze, P., Kudlacek, O., Freissmuth, M., Singer, E.A., Sitte, H.H., 2001. Oligomerization of the human serotonin transporter and of the rat GABA transporter 1 visualized by fluorescence resonance energy transfer microscopy in living cells. J. Biol. Chem. 276, 3805–3810.

Scholze, P., Freissmuth, M., Sitte, H.H., 2002. Mutations within an intramembrane leucine heptad repeat disrupt oligomer formation of the rat GABA transporter 1. J. Biol. Chem. 277, 43682–43690.

Sitte, H.H., Farhan, H., Javitch, J.A., 2004. Sodium-dependent neurotransmitter transporters: oligomerization as a determinant of transporter function and trafficking. Mol. Intervent. 4, 38–47.

Soskine, M., Steiner-Mordoch, S., Schuldiner, S., 2002. Crosslinking of membrane-embedded cysteines reveals contact points in the EmrE oligomer. Proc. Natl. Acad. Sci. U.S.A. 99, 12043–12048.

Stauffer, D.A., Karlin, A., 1994. Electrostatic potential of the acetylcholine binding sites in the nicotinic receptor probed by reactions of binding-site cysteines with charged methanethiosulfonates. Biochemistry 33, 6840–6849.

Sucic, S., Bryan-Lluka, L.J., 2005. Roles of transmembrane domain 2 and the first intracellular loop in human noradrenaline transporter function: pharmacological and SCAM analysis. J. Neurochem. 94, 1620–1630.

Sucic, S., Paczkowski, F.A., Runkel, F., Bonisch, H., Bryan-Lluka, L.J., 2002. Functional significance of a highly conserved glutamate residue of the human noradrenaline transporter. J. Neurochem. 81, 344–354.

Torres, G.E., Carneiro, A., Seamans, K., Fiorentini, C., Sweeney, A., Yao, W.D., Caron, M.G., 2003. Oligomerization and trafficking of the human dopamine transporter. Mutational analysis identifies critical domains important for the functional expression of the transporter. J. Biol. Chem. 278, 2731–2739.

Vaughan, R.A., Agoston, G.E., Lever, J.R., Newman, A.H., 1999. Differential binding of tropane-based photoaffinity ligands on the dopamine transporter. J. Neurosci. 19, 630–636.

Vaughan, R.A., Gaffaney, J.D., Lever, J.R., Reith, M.E., Dutta, A.K., 2001. Dual incorporation of photoaffinity ligands on dopamine transporters implicates proximity of labeled domains. Mol. Pharmacol. 59, 1157–1164.

Visiers, I., Braunheim, B.B., Weinstein, H., 2000. Prokink: a protocol for numerical evaluation of helix distortions by proline. Protein Eng. 13, 603–606.

Wang, J.B., Moriwaki, A., Uhl, G.R., 1995. Dopamine transporter cysteine mutants: second extracellular loop cysteines are required for transporter expression. J. Neurochem. 64, 1416–1419.

Wu, X., Gu, H.H., 2003. Cocaine affinity decreased by mutations of aromatic residue phenylalanine 105 in the transmembrane domain 2 of dopamine transporter. Mol. Pharmacol. 63, 653–658.

Yamashita, A., Singh, S.K., Kawate, T., Jin, Y., Gouaux, E., 2005. Crystal structure of a bacterial homologue of Na(+)/Cl(−)-dependent neurotransmitter transporters. Nature 437, 215–223.